



## Synthesis of long group IV semiconductor nanowires by molecular beam epitaxy

T. Xu, J. Sulerzycki, J.P. Nys, G. Patriarche, B. Grandidier, D. Stievenard

### ► To cite this version:

T. Xu, J. Sulerzycki, J.P. Nys, G. Patriarche, B. Grandidier, et al.. Synthesis of long group IV semiconductor nanowires by molecular beam epitaxy. *Nanoscale Research Letters*, 2011, 6, pp.113-1-7. <10.1186/1556-276X-6-113>. <hal-00579084>

**HAL Id: hal-00579084**

**<https://hal.science/hal-00579084v1>**

Submitted on 15 Jul 2022

**HAL** is a multi-disciplinary open access archive for the deposit and dissemination of scientific research documents, whether they are published or not. The documents may come from teaching and research institutions in France or abroad, or from public or private research centers.

L'archive ouverte pluridisciplinaire **HAL**, est destinée au dépôt et à la diffusion de documents scientifiques de niveau recherche, publiés ou non, émanant des établissements d'enseignement et de recherche français ou étrangers, des laboratoires publics ou privés.



Distributed under a Creative Commons CC BY 4.0 - Attribution - International License

**NANO EXPRESS**

**Open Access**

# Synthesis of long group IV semiconductor nanowires by molecular beam epitaxy

Tao Xu<sup>1</sup>, Julien Sulerzycki<sup>1</sup>, Jean Philippe Nys<sup>1</sup>, Gilles Patriarche<sup>2</sup>, Bruno Grandidier<sup>1\*</sup>, Didier Stiévenard<sup>1</sup>

## Abstract

We report the growth of Si and Ge nanowires (NWs) on a Si(111) surface by molecular beam epitaxy. While Si NWs grow perpendicular to the surface, two types of growth axes are found for the Ge NWs. Structural studies of both types of NWs performed with electron microscopies reveal a marked difference between the roughnesses of their respective sidewalls. As the investigation of their length dependence on their diameter indicates that the growth of the NWs predominantly proceeds through the diffusion of adatoms from the substrate up along the sidewalls, difference in the sidewall roughness qualitatively explains the length variation measured between both types of NWs. The formation of atomically flat {111} sidewalls on the  $\langle 110 \rangle$ -oriented Ge NWs accounts for a larger diffusion length.

## Introduction

Semiconductor nanowires (NWs) consist of a solid rod with a diameter usually smaller than 100 nm and a length that can vary from the nanometer to the millimeter-scale depending on the technique used to synthesize the rods. Although, for the majority of the NWs, their growth is described by the vapor-liquid-solid mechanism, based on the catalytic effect of a metal seed particle, their length is mostly related to the way the chemical compounds are supplied. In chemical vapor deposition (CVD), a wide range of partial pressures for the reactive source gases can be used. As a result, Si NWs with a millimeter-scale length have been successfully synthesized with a reasonable time [1]. Conversely, when elemental compounds are supplied instead of gas precursors, as it is the case for the growth of NWs in molecular beam epitaxy (MBE), ultra high vacuum (UHV) conditions are required. The pressure in the system is around  $10^{-9}$  times smaller than in a CVD chamber and the NW length typically does not exceed a few micrometers [2,3].

As illustrated in Figure 1 for the MBE growth, the ratio between the exposed surface of a seed particle and the collection area between the seed particles is usually

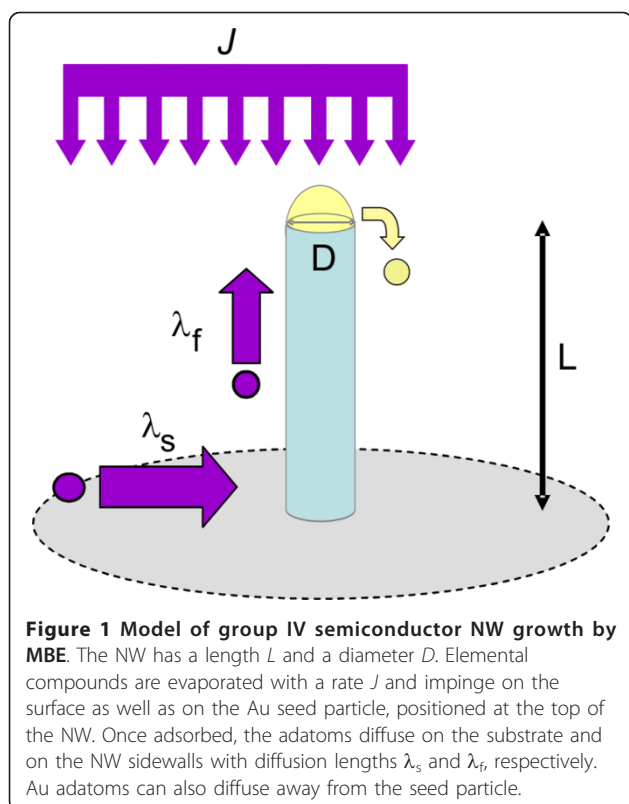
small. Due to the low pressure in the growth chamber, the direct impingement of elemental compounds onto the seed particle has a small probability to occur. Therefore, growth predominantly proceeds from the diffusion of elemental compounds that adsorb on the substrate between the seed particles. The adatoms reach the seed particles after diffusing on the substrate and the sidewalls with different diffusion length coefficients,  $\lambda_s$  and  $\lambda_f$ , respectively. As surface diffusion is a rather slow process, it is only because the crystallization at the interface between the seed particles and the NW is high enough that NWs emerge from the film growth. Such mass transport mechanism yields a NW length that is inversely proportional to the NW diameter [3,4].

In contrast to MBE grown III-V semiconductor NWs that can reach micrometer-scale lengths, group IV semiconductor NWs, which are generally grown with a  $\langle 111 \rangle$  orientation, show a much smaller length [4,5], making their integration into devices more difficult. In a purpose to understand the physical mechanisms that prevent the fabrication of group IV semiconductor NWs with micrometer-scale lengths, we investigated the growth of Si and Ge NWs on a Si(111) surface with the MBE technique. In this article, we show that not only  $\langle 111 \rangle$  but also  $\langle 110 \rangle$ -oriented Ge NWs are grown on the Si(111) surface. Surprisingly, the length of the latter can reach a few micrometers. From a comparative study of differences in the structural morphology between

\* Correspondence: bruno.grandidier@isen.fr

<sup>1</sup>Département ISEN, Institut d'Electronique, de Microélectronique et de Nanotechnologie, IEMN (CNRS, UMR 8520), 41 bd Vauban, 59046 Lille Cedex, France

Full list of author information is available at the end of the article



$\langle 111 \rangle$  and  $\langle 110 \rangle$ -oriented NWs, we are able to explain why  $\langle 110 \rangle$ -oriented NWs grow longer.

### Experimental details

The SiNWs were fabricated by the MBE method using gold droplets. The gold droplets were formed directly by gold deposition on a heated Si(111) surface in UHV at a gold deposition pressure of  $6 \times 10^{-10}$  mbar. The density and the diameter of the gold droplets are determined by the Au evaporation rate and the temperature of the samples via the Ostwald ripening process [6]. In the next step, the growth of the NWs was achieved from the sublimation of Si or Ge at a deposition pressure of  $10^{-9}$  mbar. In order to grow the NWs, the Si(111) surface was heated either at  $550^\circ\text{C}$  for the growth of Si NWs or at  $350^\circ\text{C}$  to obtain Ge NWs. The evaporation rate of elemental Si and Ge was measured from the thickness of the two-dimensional film grown on the substrate during the NW growth.

The morphology of the NWs was investigated by electron microscopies: scanning electron microscope (SEM) and high-resolution transmission electron microscope (HRTEM). To perform the HRTEM experiments, the NWs were cleaved with micromanipulators in the chamber equipped with a focus ion beam machine and transfer into holey grids covered with a very thin carbon layer.

### Results and discussion

Tilted views of the post-growth Si(111) surfaces are shown in Figure 2. When Si is sublimated, the majority of the Si NWS are found to be perpendicular to the Si (111) surface (Figure 2a). Their growth axis is thus along the  $[111]$  direction, in agreement with previous observations [4,5]. In contrast, the growth of Ge NWs leads to two different kinds of growth directions (Figure 2b). The shortest NWs usually show the Au seed particle just above the overgrown Ge film. These NWs appear normal to the surface when observed in top view SEM images such as the one shown in the inset of Figure 3. They thus grow along the  $[111]$  direction, likewise the Si NWs. As for the second type of Ge NWs, these NWs are much longer and point at  $54.7^\circ$  from the surface plane. In the top view SEM image of Figure 3, these inclined Ge NWs are found to grow along three different directions only. When projected in the (111) surface plane, the directions make an angle of  $60^\circ$ . Therefore, these Ge NWs are oriented along one of the equivalent  $\langle 110 \rangle$  directions, in agreement with the

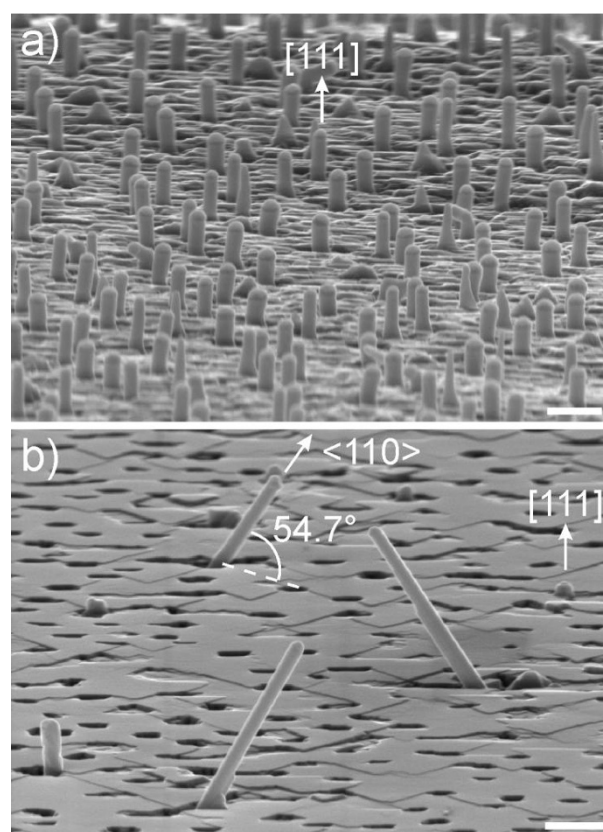
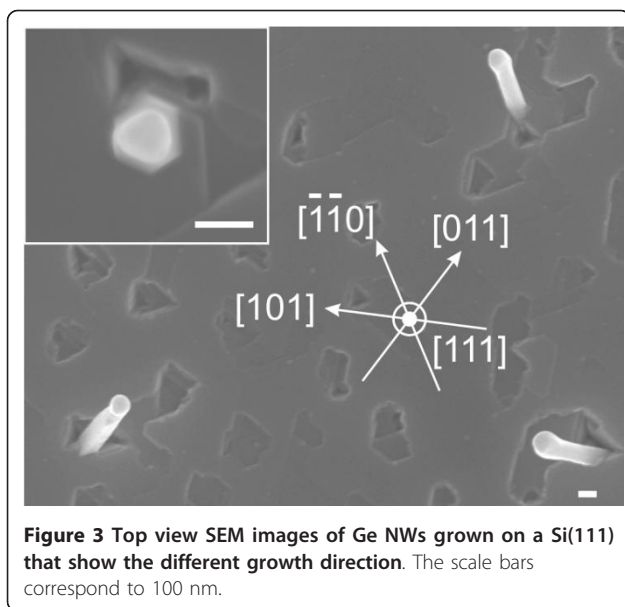


**Figure 2 SEM images of (a) Si NWs and (b) Ge NWs grown on a Si(111) surface by MBE.** The orientations of the NWs are indicated in the SEM images. The growth times were 2 and 1 h for the Si and Ge NWs, respectively. The scale bars correspond to 400 nm.



growth of  $\langle 110 \rangle$ -oriented Ge NWs obtained on the Ge (111) surface by MBE [7].

Group IV semiconductors NWs have been found to grow with different orientations, depending on the temperature of the surface during the growth and the evaporation rate of elemental Si or Ge. While a high surface temperature favors the growth of  $\langle 111 \rangle$ -oriented NWs, contradictory results have been obtained regarding the effect of the evaporation rate [7,8]. However, consistent with these previous studies, we note that the comparison of the length between the  $\langle 111 \rangle$ -oriented Ge NW and those oriented along the  $\langle 110 \rangle$  directions shows a strong difference. In our study, the first types of NWs are rarely higher than the overgrown Ge layer, while for the second type of NWs, the part of the NWs that surpasses the overgrown Ge layer can reach a length of 2  $\mu\text{m}$  when the growth time is 60 min and the deposition rate is about 1.7  $\text{\AA}/\text{s}$ . The growth direction of the NWs thus seems to play an important role on the maximum length that group IV semiconductor NWs can reach. Although the deposition rate of Si was 0.5  $\text{\AA}/\text{s}$  in Figure 2a, a two-hour growth does not allow to build NWs higher than 400 nm, consistent with previous results that reported the difficulties to grow  $\langle 111 \rangle$ -oriented Si NWs longer than 500 nm by MBE [9].

In order to understand the physical origin of the growth direction dependence on the NW length, we examined the sidewalls of both types of NWs, as shown in Figure 4. The  $\langle 111 \rangle$ -oriented Si NWs consist of six sidewalls that exhibit small facets. It has been shown that these sidewalls correspond to  $\{112\}$  planes [9]. For  $\langle 111 \rangle$ -oriented Si NWs grown by CVD at low silane partial pressure, that show similar sidewall orientations

[10], gold is known to diffuse from the seed particle and to wet the sidewalls [11,12]. Adsorption of gold on Si (112) planes is also known to cause the faceting of these planes [13]. Similarly, Au diffusion from the seed particle is at the origin of the facet formation on the  $\{112\}$  planes, for which the crystallographic orientations alternate between  $\{111\}$  planes and high index planes [14]. HRTEM images of the sidewalls for the MBE grown Si NWs are consistent with the observations performed on  $\langle 111 \rangle$ -oriented Si NWs grown by CVD. For example, Figure 4a2 reveals the rough morphology of one of the  $\{112\}$  sidewalls. Although the facets are rather rounded, probably due to the oxide layer that covered the sidewall, a corrugation of up to 2 nm is found when the height profile of the sidewall is measured.

As for the  $\langle 110 \rangle$ -oriented Ge NWs, they also exhibit an irregular hexagonal cross-section, but the orientations of the sidewalls are different. They consist of  $\{111\}$  and  $\{100\}$  planes, where two  $\{100\}$  planes are opposite to each other and are separated on each side by two adjacent  $\{111\}$  planes [15,16]. In addition, the  $\{100\}$  planes are usually narrower than the  $\{111\}$  planes and their width decreases toward the base of the NWs, which undergoes the longest exposure time to the Ge deposition and diffusion (Figure 4b1). As the  $\{111\}$  planes are the dominant sidewalls, these sidewalls were investigated by HRTEM. Figure 4b2 shows that the  $\{111\}$  sidewalls are atomically flat. Scattered bright clusters are also seen superimposed to the atomic lattice and indicate the presence of Au-rich clusters.

Similarly to the  $\langle 111 \rangle$ -oriented Si NWs, gold diffuses from the seed particle to wet the sidewalls of the  $\langle 110 \rangle$ -oriented Ge NWs. However, in contrast to the adsorption of gold on the  $\{112\}$  planes, the adsorption of gold on the Si and Ge (111) surfaces does not produce a roughening of the surface. Instead, atomically flat (111) surfaces are generally observed with a  $\sqrt{3} \times \sqrt{3}$  reconstruction, when the Au coverage is higher than one monolayer [17-19]. Our observation of a flat sidewall is thus consistent with previous surface studies about the adsorption of gold on group IV semiconductor (111) surfaces. In addition, as the  $\{111\}$  sidewalls contain Au-rich clusters, we might expect to have more than one monolayer of gold adsorbed on the NW sidewalls. Such result suggests that the formation of a  $\sqrt{3} \times \sqrt{3}$  reconstruction between the clusters occurs during the NW growth in UHV.

As already described in the introduction, the growth of NWs by MBE predominantly proceeds through the diffusion of adatoms that adsorb on the substrate in between the NWs. Indeed, if we consider the surface of the seed particle exposed to the flux of elemental compounds and the area surrounding the NWs that serves as a reservoir to collect adatoms for the NW growth,



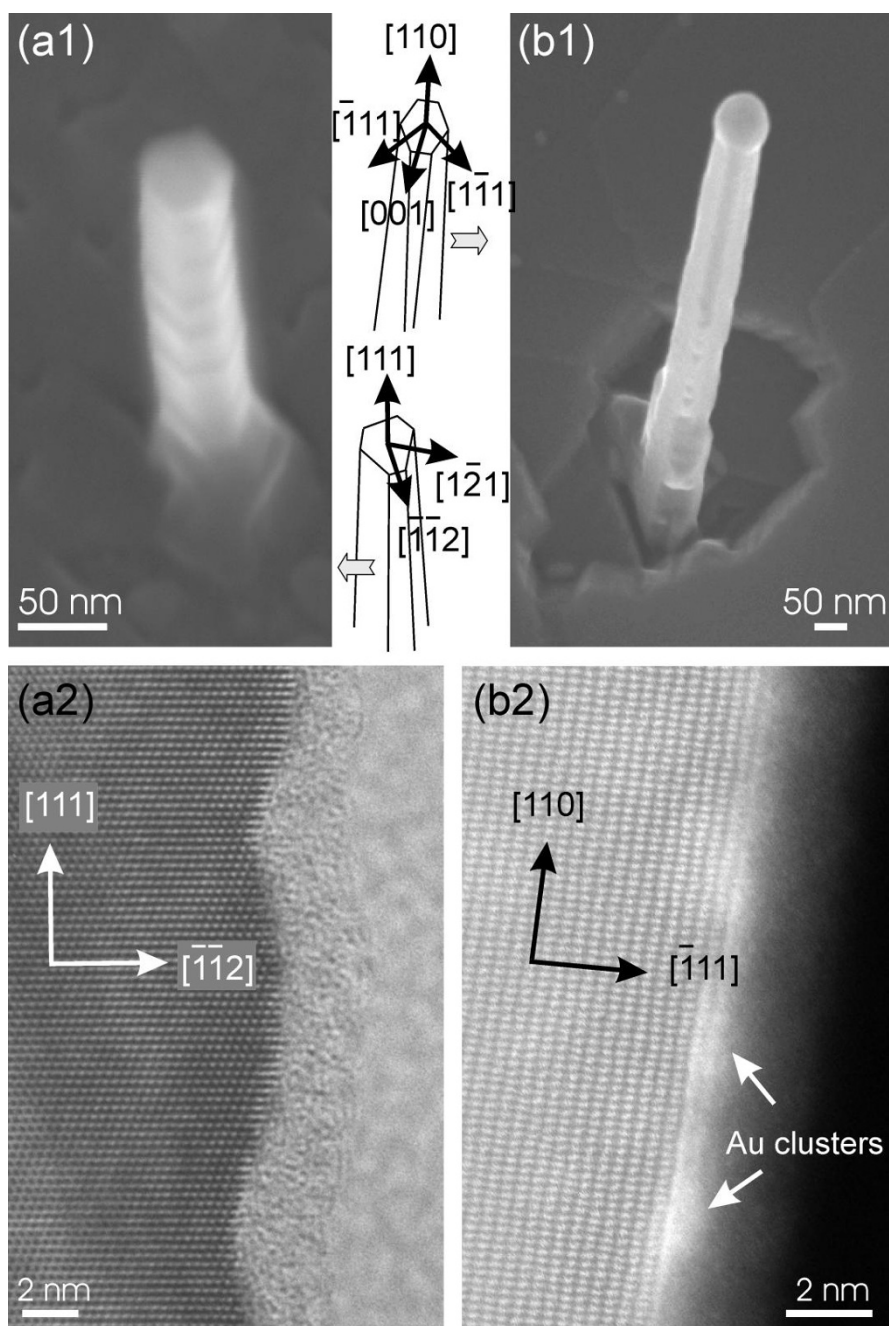
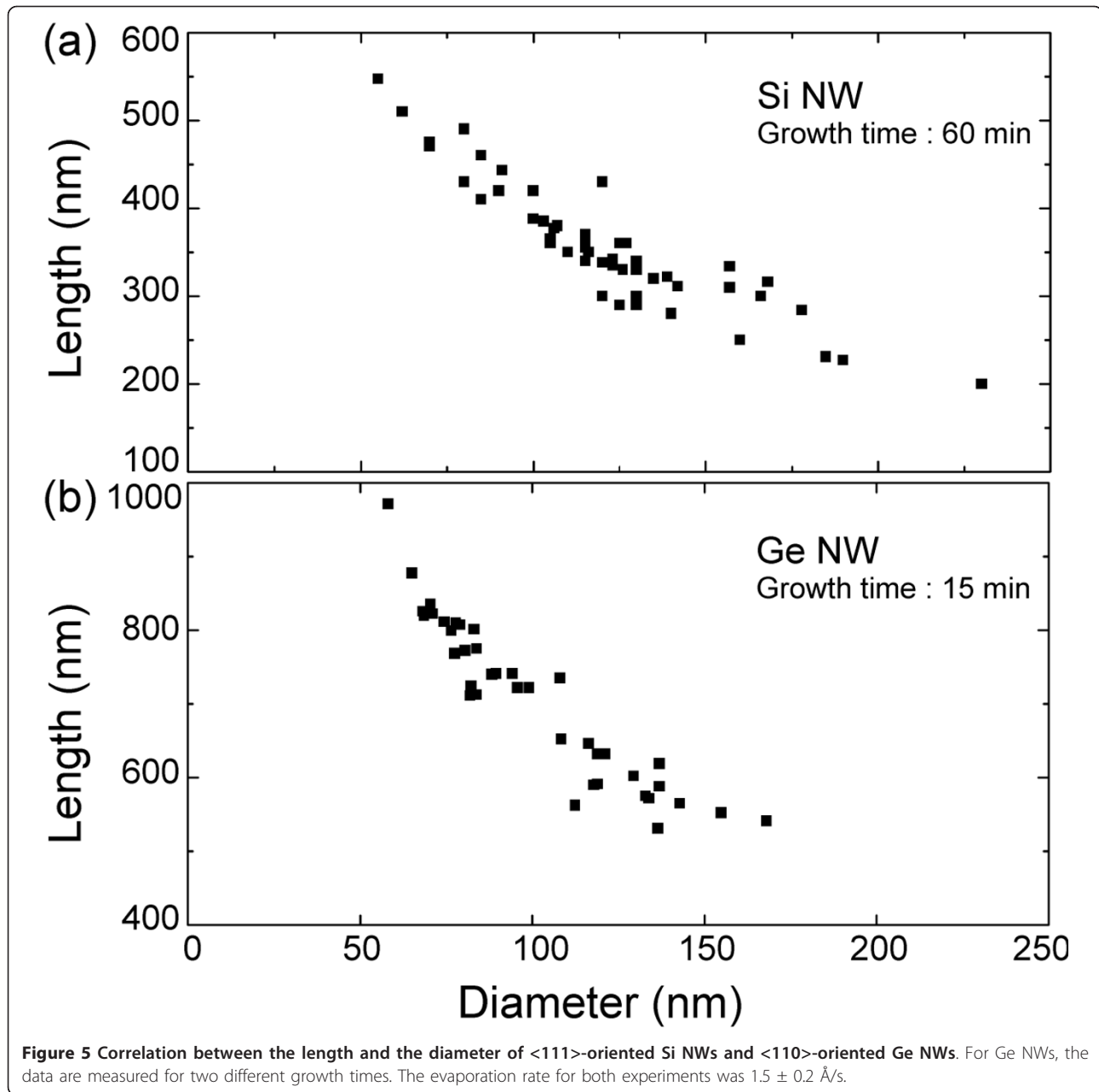


**Figure 4** SEM observation of NW sidewalls for (a1) a  $\langle 111 \rangle$ -oriented Si NWs and (b1) a  $\langle 110 \rangle$ -oriented Ge NWs grown on a Si(111) surface by MBE. Some sidewall orientations are indicated for both types of NWs. Lattice-resolved TEM images showing the roughness of (a2) a  $\{112\}$  sidewall on a  $\langle 111 \rangle$ -oriented Si NWs and (b2) a  $\{111\}$  sidewall on a  $\langle 110 \rangle$ -oriented Ge NWs.

their ratio is usually quite small. When the NW is still short, typically at the beginning of the growth, the contribution of the adatoms diffusing from the substrate up along the NW is thus the strongest to the growth rate. This mechanism implies that the crystallization rate at the interface between the seed particle and the NW is related to the flow of diffusing adatoms that become

incorporated when they reach the circumference of the interface [4]. It yields a characteristic signature: the NW length varies like the inverse of the diameter. Such a behavior appears in Figure 5a for the case of the  $\langle 111 \rangle$ -oriented Si NWs grown by MBE.

It is also visible after a 15 min for the growth of  $\langle 110 \rangle$ -oriented Ge NWs (Figure 5b). Although the



deposition rate was almost similar, comparison of the maximum length that can be reached between the  $\langle 111 \rangle$  and  $\langle 110 \rangle$ -oriented NWs clearly shows that the  $\langle 110 \rangle$ -oriented NWs are quickly much longer. Based on the mass transport model described in [20], in the case of NWs that are still short, the length growth rate dependence on the adatoms diffusing onto the sidewalls from the substrate toward the interface between the Au droplet and the NW is expressed as follows:

$$\frac{dL}{dt} = \frac{4\Omega|J|}{D \cosh(L/\lambda_f)} \quad (1)$$

where  $\Omega$ ,  $J$ , and  $\lambda_f$  are, respectively, the atomic volume of the growth species, the flow of adatoms from the substrate toward the NW sidewalls, and the diffusion length along the NW sidewalls. Considering that  $\Omega$  and  $J$  do not significantly vary between the growth of Si and Ge NWs, for a given diameter, the length growth rate is found to vary as the inverse of a cosh function that depends on  $\lambda_f$ . A higher diffusion length on the sidewalls results in an increase of the length growth rate.

Surface diffusion requires overcoming an energy barrier [21]. The smaller the surface corrugation is, the lower the activation energy is. For a given time, elemental Si or Ge can thus diffuse further away from their adsorption site

when the surface is atomically flat [22]. The longest diffusion length found for the case of  $\langle 110 \rangle$ -oriented Ge NWs is, therefore, consistent with atomically flat  $\{111\}$  sidewalls in comparison with the rough-faceted  $\{112\}$  sidewalls of the  $\langle 111 \rangle$ -oriented NWs.

When  $L$  becomes larger than  $\lambda_f$ , then the length growth rate depends mainly on the diffusion of adatoms that adsorb directly onto the NW sidewalls or on the seed particle. Therefore, the NWs with the smallest diameters grew slower while the NWs with the biggest diameters keep on growing with the same length growth rate. The effect of a limited diffusion length is readily visible in Figure 6. While the  $\langle 110 \rangle$ -oriented Ge NWs appear cylindrical at the beginning of the growth (Figure 6a), some of the  $\{111\}$  sidewalls may show a change of their morphology, as the growth proceeds. Such an example is seen in Figure 6b, where a strong overgrowth occurs at the base of the NW indicating that the adatoms from the substrate are rather incorporated onto the sidewalls than diffusing up to the top of the NWs. Finally, when the growth duration approaches tens of minutes, Au may have completely diffused away from the original seed particle. As a result, the NW cannot grow in length any more, but overgrowth on the sidewalls occurs. The  $\{100\}$  sidewalls, for which the surface tension is higher [15,23], disappear through the lateral growth of the  $\{111\}$

sidewalls, giving rise to a typical rhombohedral cross-section (Figure 6c).

In summary, by combining SEM and TEM analysis of group IV semiconductor NWs grown by MBE on a Si (111) surface, the structural properties of Si and Ge NWs with different growth axes have been investigated. As gold diffuses from the seed particle during the growth and wets the NW sidewalls, a significant change of the sidewall roughness can occur depending on the sidewall orientations. The roughness strongly affects the diffusion length of the diffusing Si or Ge adatoms toward the interface between the seed particle and the NW, and prevents the growth of NWs with micrometer-scale lengths. A good control of the NW growth axis is, therefore, important to obtain sidewalls with the lowest surface tension.

#### Abbreviations

CVD: chemical vapor deposition; HRTEM: high-resolution transmission electron microscope; MBE: molecular beam epitaxy; NWs: nanowires; SEM: scanning electron microscope; UHV: ultra high vacuum.

#### Acknowledgements

We thank D. Troade for the manipulation of the Ge NWs onto the TEM grid. The authors acknowledge financial support from the DGA (Direction Générale de l'Armement) under contract REI-N02008.34.0031.

#### Author details

<sup>1</sup>Département ISEN, Institut d'Electronique, de Microélectronique et de Nanotechnologie, IEMN (CNRS, UMR 8520), 41 bd Vauban, 59046 Lille Cedex,

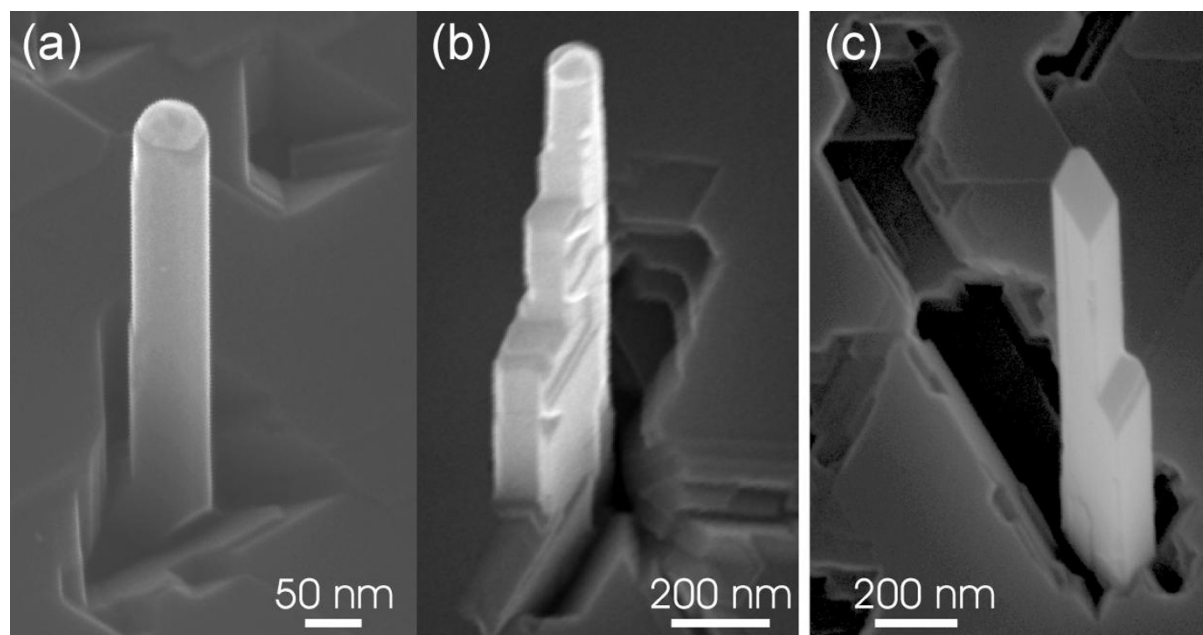


**Figure 6 Evolution of the  $\langle 110 \rangle$ -oriented Ge NW morphology.** The NWs initially show (a) an irregular hexagonal cross-section, then (b) a reduction of the gold seed particle and a lateral overgrowth on the  $\{111\}$  sidewall that is exposed to the Ge flux, and finally (c) the disappearance of both the gold seed particle and the  $\{100\}$  sidewalls, giving rise to Ge NW with a rhombohedral cross-section.

France <sup>2</sup>CNRS-Laboratoire de Photonique et de Nanostructures, Route de Nozay, 91460 Marcoussis, France

#### Authors' contributions

TX, JPN, BG designed the experiments, TX, JS, JPN performed the experiments, GP performed the TEM analyses, BG wrote the paper. All authors discussed the results and commented on the manuscript.

#### Competing interests

The authors declare that they have no competing interests.

Received: 20 September 2010 Accepted: 2 February 2011

Published: 2 February 2011

#### References

1. Park W II, Zheng G, Jiang X, Tian B, Lieber CM: Controlled synthesis of millimeter-long silicon nanowires with uniform electronic properties. *Nano Lett* 2008, **8**:3004.
2. Plante MC, LaPierre RR: Growth mechanisms of GaAs nanowires by gas source molecular beam epitaxy. *J Cryst Growth* 2006, **286**:394.
3. Dubrovskii VG, Cirilin GE, Soshnikov IP, Tonkikh AA, Sibirev NV, Samsonenko YB, Ustinov YB: Diffusion-induced growth of GaAs nanowhiskers during molecular beam epitaxy: Theory and experiment. *Phys Rev B* 2005, **71**:205325.
4. Schubert L, Werner P, Zakharov ND, Gerth G, Kolb FM, Long L, Gösele U, Tan TY: Silicon nanowhiskers grown on (111) Si substrates by molecular-beam epitaxy. *Appl Phys Lett* 2004, **84**:4968.
5. Dujardin R, Poydenot V, Devillers T, Favre-Nicolin V, Gentile P, Barski A: Growth mechanism of Si nanowhiskers and SiGe heterostructures in Si nanowhiskers: X-ray scattering and electron microscopy investigations. *Appl Phys Lett* 2006, **89**:153129.
6. Xu T, Nys JP, Grandidier B, Stiévenard D, Coffinier Y, Boukherroub R, Larde R, Cadel E, Pareige P: Growth of Si nanowires on micropillars for the study of their dopant distribution by atom probe tomography. *J Vac Sci Technol B* 2008, **26**:1960.
7. Kramer A, Albrecht M, Boeck T, Remmele T, Schramm P, Fornari R: Self-assembled and ordered growth of silicon and germanium nanowires. *Superlatt Microstruct* 2009, **46**:277.
8. Irrera A, Pecora EF, Priolo F: Control of growth mechanisms and orientation in epitaxial Si nanowires grown by electron beam evaporation. *Nanotechnology* 2009, **20**:135601.
9. Werner P, Zakharov ND, Gerth G, Schubert L, Gösele U: On the formation of Si nanowires by molecular beam epitaxy. *Int J Mater Res* 2006, **97**:1008.
10. Ross FM, Tersoff J, Reuter MC: Sawtooth Faceting in Silicon Nanowires. *Phys Rev Lett* 2005, **95**:146104.
11. Hannon JB, Kodambaka S, Ross F, Tromp RM: The influence of the surface migration of gold on the growth of silicon nanowires. *Nature* 2006, **440**:69.
12. Den Hertog M, Rouvière JL, Dhalluin F, Desré PJ, Gentile P, Ferret P, Oehler F, Baron T: Control of gold surface diffusion on Si nanowires. *Nano Lett* 2008, **8**:1544.
13. Wiethoff C, Ross FM, Copel M, Horn-von Hoegen M, Meyer zu Heringdorf F-J: Au Stabilization and Coverage of Sawtooth Facets on Si Nanowires Grown by Vapor- Liquid- Solid Epitaxy. *Nano Lett* 2008, **8**:3065.
14. Xu T, Nys JP, Addad A, Lebedev OI, Urbieta A, Salhi B, Berthe M, Grandidier B, Stiévenard D: Faceted sidewalls of silicon nanowires: Au-induced structural reconstructions and electronic properties. *Phys Rev B* 2010, **81**:115403.
15. Wu Y, Cui Y, Huynh L, Barrelet CJ, Bell DC, Lieber CM: Controlled growth and structures of molecular-scale silicon nanowires. *Nano Lett* 2004, **4**:433.
16. Hanrath T, Korgel BA: Crystallography and surface faceting of germanium nanowires. *Small* 2005, **1**:717.
17. Nagao T, Hasegawa S, Tsuchie K, Ino S, Voges C, Klos G, Pfnür H, Henzler M: Structural phase transitions of Si (111)-(√3 × √3) R30°-Au: Phase transitions in domain-wall configurations. *Phys Rev B* 1998, **57**:10100.
18. Grozea D, Bengu E, Marks LD: Surface phase diagrams for the Ag-Ge (111) and Au-Si (111) systems. *Surf Sci* 2000, **461**:23.
19. Seehofer L, Johnson RL: STM study of gold on Ge (111). *Surf Sci* 1994, **318**:21.
20. Johansson J, Svensson CPT, Mårtensson T, Samuelson L, Seifert W: Mass transport model for semiconductor nanowire growth. *J Chem Phys* 2005, **109**:13567.
21. Gomer R: Diffusion of adsorbates on metal surfaces. *Rep Prog Phys* 1990, **53**:917.
22. Mo YW, Lagally MG: Anisotropy in surface migration of Si and Ge on Si (001). *Surf Sci* 1991, **248**:313.
23. Zhang JM, Ma F, Xu KW, Xin XT: Anisotropy analysis of the surface energy of diamond cubic crystals. *Surf Interface Anal* 2003, **35**:805.

doi:10.1186/1556-276X-6-113

**Cite this article as:** Xu et al.: Synthesis of long group IV semiconductor nanowires by molecular beam epitaxy. *Nanoscale Research Letters* 2011 **6**:113.

**Submit your manuscript to a SpringerOpen<sup>®</sup> journal and benefit from:**

- Convenient online submission
- Rigorous peer review
- Immediate publication on acceptance
- Open access: articles freely available online
- High visibility within the field
- Retaining the copyright to your article

Submit your next manuscript at ► [springeropen.com](http://springeropen.com)